EISSN: 2707-0425

East African Journal of Science, Technology and Innovation, Vol. 6 (Special issue 1): December 2024

DFT and TD-DFT studies of the effect of internal acceptor based on D-A′-Π-A structure for dye-sensitized solar cells

[1]SANAMA M K., [1]ABUBAKARI I., BABU N S*

[1]Department of chemistry, The University of Dodoma, Dodoma, Tanzania

***Corresponding Author**: michaelsanama@gmail.com

Abstract

Economic growth and population expansion have led to an increase in the world's energy consumption. For human use, solar energy is one of the greatest significant renewable energy sources. In this study, six D-A′-π-A of newly organic dye molecules (M1-M6) have been developed by changing the internal acceptor groups. Density functional theory (DFT) and time-dependent DFT (TD-DFT) theory techniques through B3LYP and 6-311G basis set have been employed to assess their optoelectronic properties as well as photovoltaic characteristics of six D-A′-π-A novel organic dyes designed molecules. A number of critical factors like geometrical optimization, highest occupied molecular orbital (HOMO) and lowest unoccupied molecular orbital (LUMO) energy level, energy bandgap and light-harvesting efficiency (LHE) have been studied so as to determine the effect of developed internal acceptor group on increasing intramolecular charge transfer (ICT) and improving light-absorbing capacities. From the data, out of all the developed six organic dye molecules, M2 perform better than other organic dye molecules, showing injection driving force (ΔGinject) of -0.1807 eV and -0.1125 eV for gas phase and solvent phase, respectively, open-circuit voltage (Voc) of 0.3003 eV and 0.2516 eV for gas phase and solvent phase, respectively, and maximum absorption wavelength of 959.76 nm and 1148.69 nm for gas phase and solvent phase, respectively. Therefore, M2 dye molecule was observed to be more favorable candidate in the application of dye-sensitized solar cells (DSSCs) technology hence recommended for practical study to offer effective advancement in D-A′-π-A system organic dye for sustainable energy development. Additionally, this study contributes to directing researchers for further study toward designing more effective novel organic dye molecules for DSSCs application.

Keywords: *D-A′-π-A; DFT; Dye-sensitized solar cells; Optoelectronic properties; Photovoltaic properties; TD-DFT*

Received: 18/06/24
Accepted: 05/12/24
Published: 20/12/24

Cite as, *Sanama et al., (2024)*. DFT and TD-DFT studies of the effect of internal acceptor based on D-A′-Π-A structure for dye-sensitized solar cells. *East African Journal of Science, Technology and Innovation 6 (Special issue 1).*

Introduction

The world's energy output needs to be drastically altered in order to sustain the growing energy demand and resolve the environmental challenges brought on by use of fossil fuels which are diminishing and poses significant hazards to the environment and public health (Hosseinnezhad *et al*., 2020). These challenges call for swift shift toward the widespread expenditure of renewable energy sources, requiring quick thinking and well-coordinated effort. Solar energy stands out as a viable and advantageous substitute for traditional fossil

fuels since it is environmentally friendly and clean (Prajapat *et al.,* 2023). Additionally, it is due to enormous potential of solar energy, which is several times greater than the world's current energy consumption (Dindorkar and Yadav, 2022).

The most extensively utilized solar energy technology available today is silicon-based solar cells with monocrystalline, polycrystalline or amorphous designs (Hachi *et al.,* 2020). However, the exorbitant cost of producing these devices continues to be the main barrier to their widespread use. As a result, dye-sensitized solar cells (DSSCs) are informed to remain the best alternative because of their extraordinary power conversion efficiency (PCE) as well as low cost of production (Janjua, 2021). The DSSC operation principally involves four key components: semiconductors, dye molecule's electrodes, electrolytes and dye molecule which is responsible for absorption of solar radiation and acts as a source of electrons for the cell. The technology utilizes both natural and synthetic dye molecules even though due to climatic change mitigation strategies, the natural dyes have been discourage with promotion of synthetic ones due to excessive deforestation (Pizzicato *et al.,* 2023).

The two categories of synthetic dyes frequently utilized in DSSCs are metal-based complexes and metal-free organic dyes. Due to extraordinary cost of metals, its scarcity their toxicity to environment and the low synthetic yield (Huang *et al.,* 2016; Saad Ebied *et al.,* 2022), the current researchers focus on developing metal-free organic dyes following their environment friendliness, high molar extinction coefficient, easy of synthesis and purification, low cost and structural flexibility (Janjua *et al.,* 2021). Several systems has been developed based on metal-free organic dyes centered on conjugate system which couples one or more donor (D) as well as acceptor (A) units to create the D-A and D-π-A structure that accounts for the majority of the most efficient organic dyes (Sharmoukh *et al.,* 2020). Other potential artificial sensitizer combinations such as D-π-A-A, D-D-π-A, D-A-π-A and D-$(\pi\text{-A})_2$ (Tripathi *et al.,* 2020), have also been identified and have a notable benefit due to their high efficiency (Wu *et al.,* 2019).

The widely studied D-π-A system is restricted by its inability to absorb solar energy hence to maximize its performance additional acceptor segments must be added to the D-π-A configuration to create the D-A-π-A structure (Liu *et al.,* 2017). Numerous benefits of the D-A-π-A system like its UV-visible absorption band, ease of adjusting the molecular energy gap, effective intramolecular charge transfer, reduction of electron recombination, generation of red-shift of the absorption band, elimination of aggregation as well as increased solar stability and efficiency have drawn extensive research attention (Arslan *et al.,* 2021; Chaitanya *et al.,* 2017; Li *et al.,* 2019).

Therefore, this study aimed at developing new organic dye molecule through investigating the effect of internal acceptor (A') of D-A'-π-A for DSSCs application using quantum chemical methods. The study was carried out by substituting six internal acceptors: benzo[c][1,2,5]oxadiazole, benzo[c][1,2,5]thiadiazole, [1,2,5[oxadiazole[3,4,c]pyridine, [1,2,5]thiadiazole[3,4,c]pyridine, [1,2,5]oxadiazole[3,4,d]pyridazine and [1,2,5]thiadiazole[3,4,d]pyridazine to the D-A'-π-A to develop six different molecules named M1, M2, M3, M4, M5 and M6 respectively.

Materials and Methods

Molecular design and Computational details

In this study, six newly organic dyes molecules founded on D-A'-π-A system were designed by varying internal acceptor using benzo[c][1,2,5]oxadiazole, benzo[c][1,2,5]thiadiazole, [1,2,5]oxadiazole[3,4-c]pyridine, [1,2,5]thiadiazole[3,4-c]pyridine, [1,2,5]oxadiazole[3,4-d]pyridazine and [1,2,5]thiadiazole[3,4-d]pyridazine here referred as A'1, A'2, A'3, A'4, A'5 and A'6, respectively, to the constant donor, π-spacer and external acceptor as shown in Figure 1a. The design was done by substituting the internal acceptors A'1, A'2, A'3, A'4, A'5 and A'6 to form dye molecules M1, M2, M3, M4, M5 and M6, respectively, as presented in Figure 1b. The designed dye

molecules were studied utilizing DFT and TD-DFT methods utilizing Gaussian 09 program (Frisch *et al.,* 2015) through B3LYP hybrid function as well as 6-311G basis set in gas and solvent phases. The ground state geometries were painstakingly tuned without symmetry limitations utilizing DFT method while TD-DFT was used to investigate the molecules in excited state. The conductor-like polarizable continuum (CPCM) model was employed towards incorporate the impact of solvent at both DFT and TD-DFT theoretical level using acetonitrile solvent.

Figure 1

(a) The donor, internal acceptors, π-spacer and external acceptor used to design D-A′-π-A dye molecules (b) The molecular design strategy for dye molecules M1 to M6

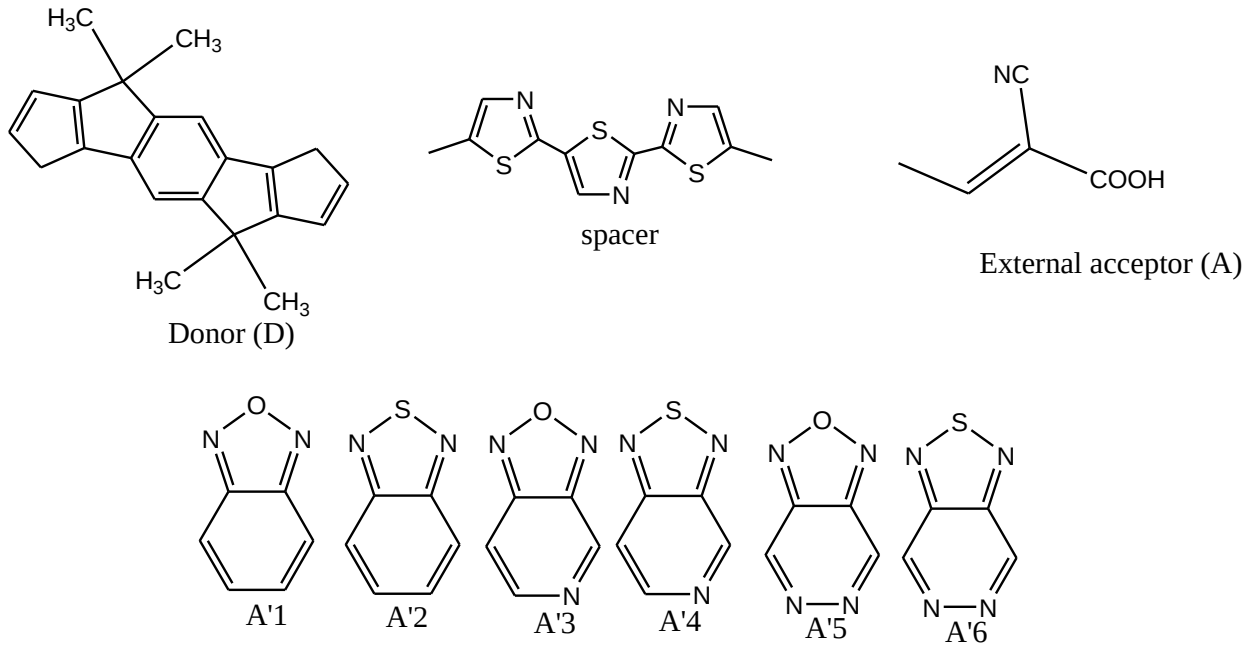

(a)

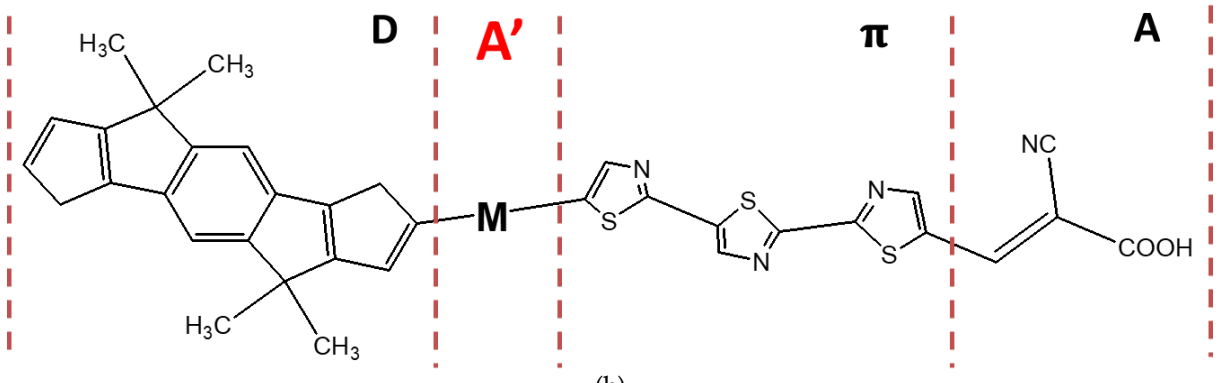

(b)

Theoretical calculation

For critical evaluation of the studied molecules different parameters were computed. To evaluate photovoltaic performance of molecules, the open circuit voltage (V_{OC}) was calculated using an analytical relationship based on equation (1) (T. Zhang *et al.,* 2014)

$$V_{oc} = E_{LUMO} - E_{CB} \quad (1)$$

Whereas E_{LUMO}, indicates the LUMO energy level of the dye and E_{CB}, indicates the energy of the conduction band of TiO_2 (E_{CB} = -4.0 eV) (Singh, 2012). The light harvesting efficiency (LHE) which have an impact on DSSC absorption performance was calculated using equation (2) (Sharmoukh *et al.,* 2018).

$$LHE = 1 - 10^{-f} \quad (2)$$

Where f represents the oscillator strength in relation to the dye's maximum wavelength (λ_{max}). Another parameter which tells injection power of dye is injection driving force ($\triangle G^{inject}$) which was calculated using equation (3) (Katoh *et al.,* 2004).

$$\triangle G^{inject} = E^{dye*} - E_{CB} \quad (3)$$

Where E_{CB} represents the reduction potential of the TiO_2 conduction and E^{dye*} donates the oxidation potential energy molecule in the excited state and it was the value of E^{dye*} determined using the equation (4) (Al-Masoodi1 *et al.,* 2021).

$$E^{dye*} = E^{dye} - E^{00} \quad (4)$$

Whereas E^{dye} represents the oxidation state of the molecule in ground state and is considered as -E_{HOMO} and E^{00} indicates the vertical transition energy parallel to the λ_{max} (Kacimi *et al.,* 2020). The dye regeneration force ($\triangle G_{reg}$) which indicates the driving force for dye regeneration was calculated using equation (5), indicates the driving force for dye regeneration (Pounraj, 2018).

$$\triangle G_{reg} = E^{dye} - E^{redox} \quad (5)$$

Where E^{redox} is represented by the electrolyte's redox potential (-4.8 eV) (Singh and Ravindra, 2012).

Results

The study involved the optimization of six organic dye molecules centered on D-A'-π-A system. The structure for optimized organic dye molecules are presented in Figure 2 for solvent phase as representative, and the trends were observed similar even in the gas phase. To demonstrate the conformation of optimized dye molecules the dihedral angle was considered as a geometrical parameter to assess it and presented in Table 1.

Figure 2

The optimized structure of all studied dye molecules in solvent phase.

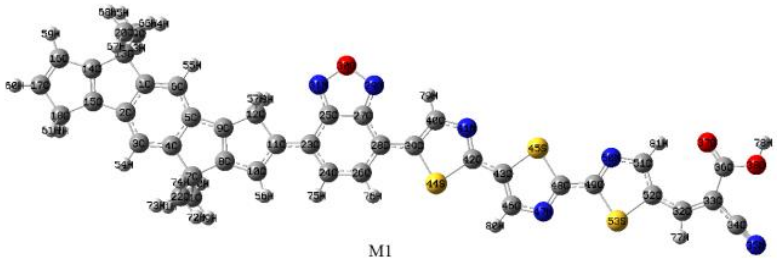

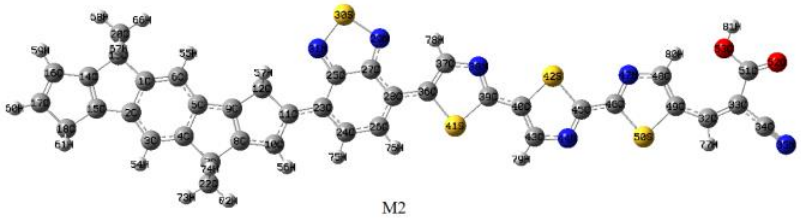

M2

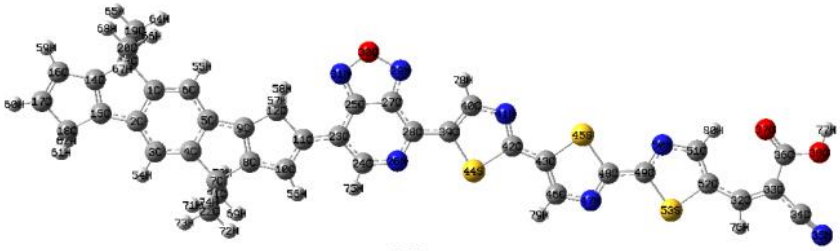

M3

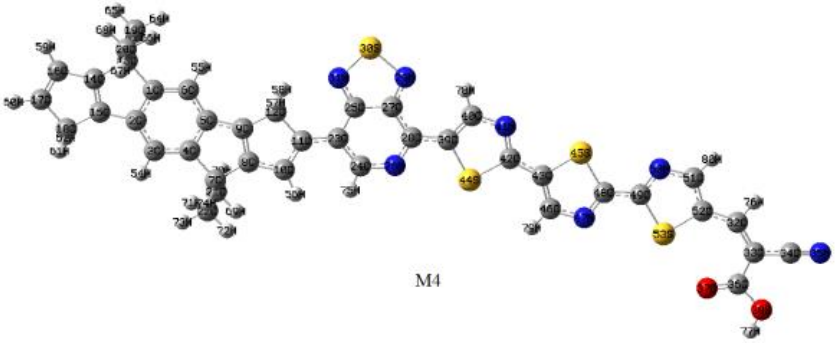

M4

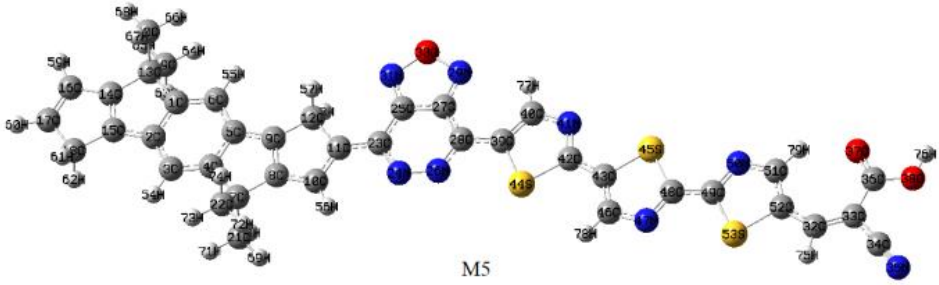

M5

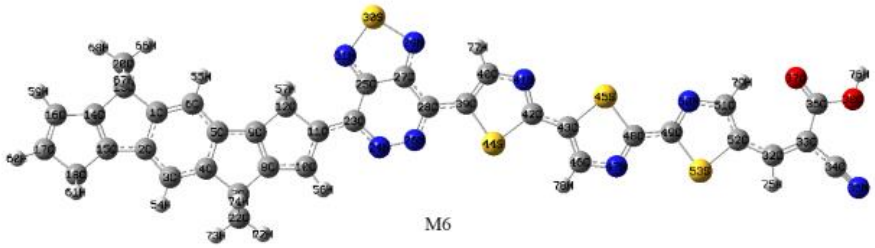

M6

Table 1

The selected optimized dihedral angles of all studied molecules in gas and solvent phases.

Gas phase						
Molecules	D-A′		A′-π		π-A	
	ANGLE	DEGREE	ANGLE	DEGREE	ANGLE	DEGREE
MI	C12-C11-C23-C24	179.99	C26-C28-C39-C40	179.99	S53-C52-C32-C33	179.99
M2	C12-C11-C23-C24	179.99	C26-C28-C36-C37	179.99	S50-C49-C32-C33	179.97
M3	C12-C11-C23-C24	179.99	N26-C28-C39-C40	179.99	S53-C52-C32-C33	179.99
M4	C12-C11-C23-C24	179.97	N26-C28-C39-C40	179.99	S53-C52-C32-C33	179.99
M5	C12-C11-C23-N24	179.99	N26-C28-C39-C40	179.99	S53-C52-C32-C33	179.99
M6	C12-C11-C23-N24	179.99	N26-C28-C39-C40	179.98	S53-C52-C32-C33	179.98
Solvent phase						
MI	C12-C11-C23-C24	179.99	C26-C28-C39-C40	179.99	S53-C52-C32-C33	180.00
M2	C12-C11-C23-C24	179.98	C26-C28-C36-C37	179.99	S50-C49-C32-C33	179.94
M3	C12-C11-C23-C24	179.99	N26-C28-C39-C40	179.99	S53-C52-C32-C33	179.99
M4	C12-C11-C23-C24	179.97	N26-C28-C39-C40	179.99	S53-C52-C32-C33	179.99
M5	C12-C11-C23-N24	179.99	N26-C28-C39-C40	179.99	S53-C52-C32-C33	179.99
M6	C12-C11-C23-N24	180.00	N26-C28-C39-C40	179.99	S53-C52-C32-C33	179.99

This work involved the contour plots of HOMO and LUMO diagrams of all investigated six organic dye molecules based on the D-A′π-A as computed in both gas and solvent phases. As representative, the diagrams computed in solvent phase are presented in the Figure 3 as similar trends were also observed in a gas phase. The presented HOMO and LUMO diagrams used to assess the transferring of electron from the group that donates electron to the group that accepts electron with the assistance of bridges.

Figure 3

The HOMO and LUMO diagrams of the investigated dye molecules in solvent phase

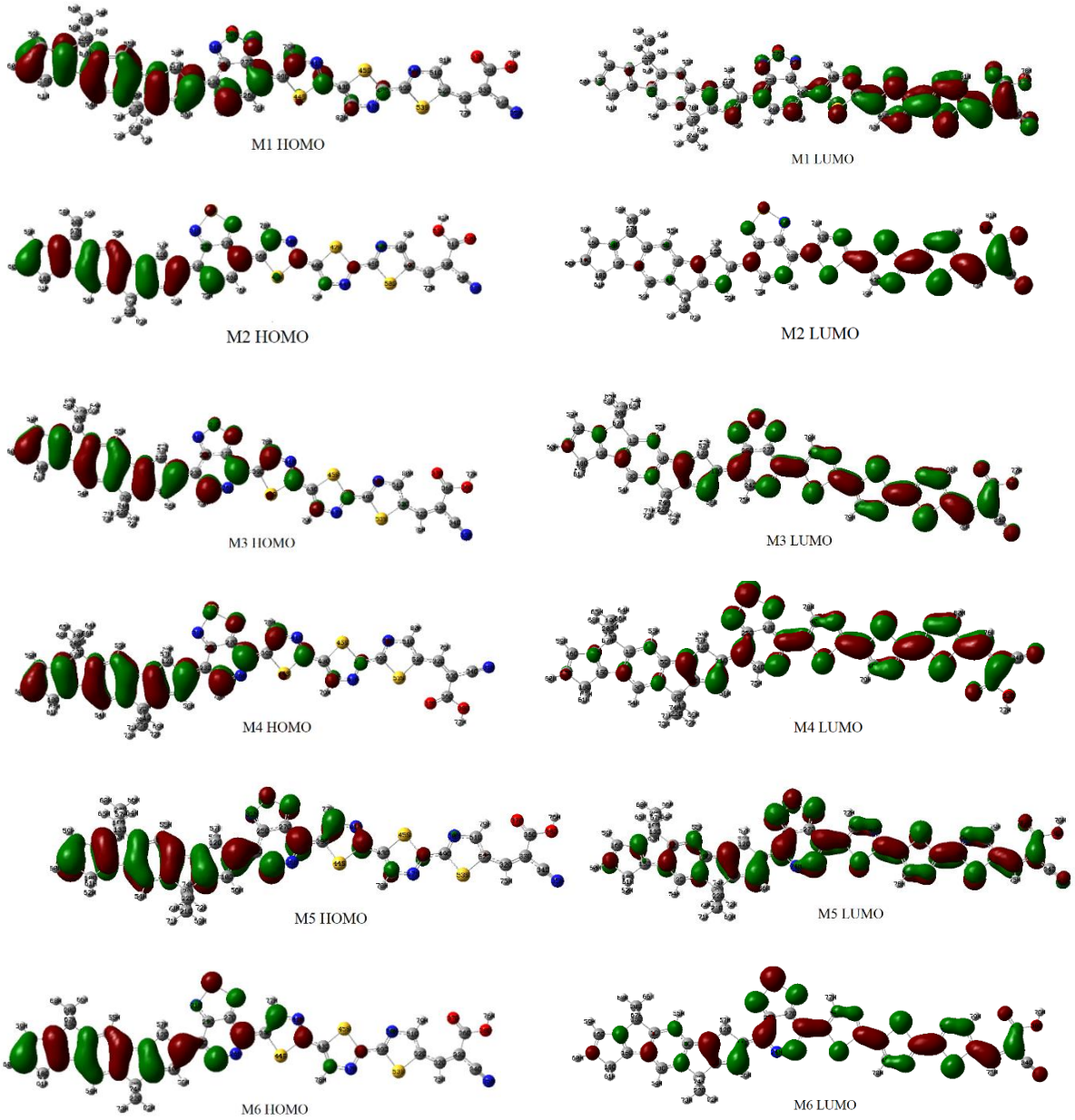

Absorption properties of all investigated six organic dye molecules with D-A′-π-A system were considered in this study. The absorption spectra for the molecules are presented in the Figure 4a and b for gas phase and solvent phase, respectively. To demonstrate the performance of all investigated six organic dye molecules in absorption of solar light, absorption intensity and absorption wavelength were considered.

Figure 4

The simulated absorption spectra of all investigated dye molecules in (a) gas phase and (b) solvent phase

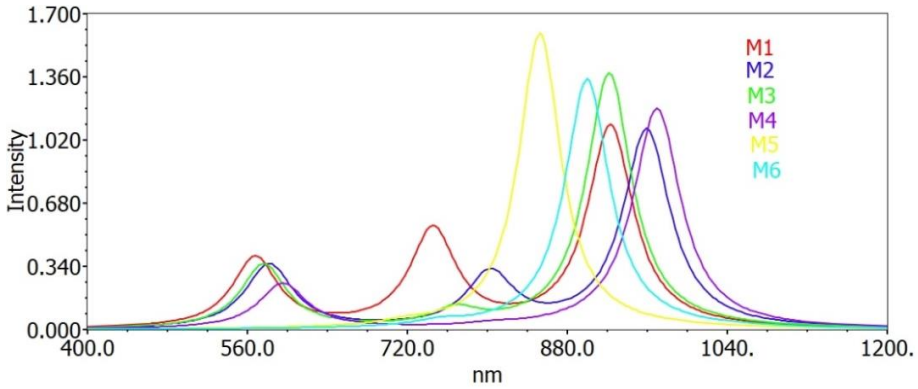

(a)

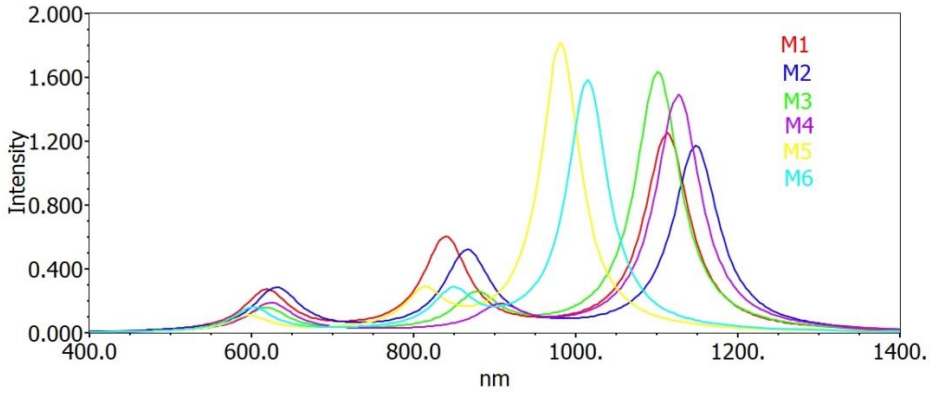

(b)

Moreover, the study considered some parameters that can be used to evaluate the electronic properties of all designed molecules. These parameters were presented in the Table 2 for gas and solvent phases. The parameters were considered in this work in order to investigate among six organic dye molecules, which dye molecule was performed better than others.

Table 2

The electronic parameters of all investigated dye molecules in the gas and solvent phases.

Gas phase				
Molecules	HOMO (eV)	LUMO (eV)	E_{gap} (eV)	μ (Debye)
M1	-5.1843	-3.7239	1.4604	15.6729
M2	-5.1111	-3.6997	1.4114	18.1707
M3	-5.2725	-3.8463	1.4262	16.5103
M4	-5.1557	-3.7726	1.3831	16.3504
M5	-5.4548	-3.9307	1.5241	17.8410
M6	-5.3536	-3.8893	1.4643	18.2094
Solvent phase				
M1	-5.0281	-3.7784	1.2542	21.6061
M2	-4.9669	-3.7484	1.2185	23.9170
M3	-5.0983	-3.8656	1.2327	24.8342
M4	-5.0316	-3.8100	1.2216	23.4206
M5	-5.2877	-3.9143	1.3734	27.4097
M6	-5.2151	-3.8678	1.3473	25.9480

The photovoltaic properties were also investigated in this study, by considering parameters that have ability to assess the ability of molecules in electricity production. The parameters are shown in the Table 3 for both gas and solvent phases.

Table 3

The calculated photovoltaic properties of all studied molecules in gas and solvent phases.

Gas phase							
Molecules	E^{00} (eV)	E^{dye} (eV)	E^{dye*} (eV)	$\triangle G^{inject}$ (eV)	$\triangle G_{reg}$ (eV)	LHE	V_{OC} (eV)
M1	1.3424	5.1843	3.8419	-0.1581	0.3843	0.9193	0.2761
M2	1.2918	5.1111	3.8193	-0.1807	0.3111	0.9153	0.3003
M3	1.3445	5.2725	3.9280	-0.0720	0.4725	0.9581	0.1537
M4	1.2782	5.1557	3.8775	-0.1225	0.3557	0.9355	0.2274

M5	1.4536	5.4548	4.0012	0.0012	0.6548	0.9748	0.0693
M6	1.3773	5.3536	3.9799	-0.0201	0.5536	0.9554	0.1107
Solvent phase							
M1	1.1139	5.0281	3.9142	-0.0858	0.2281	0.9430	0.2216
M2	1.0794	4.9669	3.8875	-0.1125	0.1669	0.9319	0.2516
M3	1.1252	5.0983	3.9731	-0.0269	0.2983	0.9766	0.1344
M4	1.1001	5.0316	3.9315	-0.0685	0.2316	0.9677	0.1900
M5	1.2629	5.2877	4.0248	0.0248	0.4877	0.9845	0.0857
M6	1.2210	5.2151	3.9941	-0.0059	0.4151	0.9734	0.1322

Figure 4a and b demonstrated the absorption spectra that can assess the ability of all studied six organic dye molecules to absorb light from the sun and Table 4 show the calculated absorption properties for the molecules in both gas and solvent phases so as to extend the further assessment about the ability of designed dyes towards solar light absorption.

Table 4

The calculated absorption spectra data of all investigated molecules in a gas phase and solvent phase.

Gas phase				
Molecules	λ_{max} (nm)	E_{ex} (eV)	F	MO Contribution
M1	923.58	1.3424	1.0930	HOMO→LUMO +1 (99.8%)
M2	959.76	1.2918	1.0719	HOMO→LUMO +1 (100%)
M3	922.17	1.3445	1.3781	HOMO→LUMO +1 (100%)
M4	969.96	1.2782	1.1903	HOMO→LUMO +1 (100%)
M5	852.96	1.4536	1.5978	HOMO→LUMO +1 (99.7%)
M6	900.22	1.3773	1.3511	HOMO→LUMO +1 (100%)
Solvent phase				
M1	1113.04	1.1139	1.2441	HOMO→LUMO +1 (100%)
M2	1148.69	1.0794	1.1666	HOMO→LUMO +1 (100%)
M3	1101.85	1.1252	1.6316	HOMO→LUMO +1 (100%)
M4	1127.04	1.1001	1.4906	HOMO→LUMO +1 (100%)
M5	981.76	1.2629	1.8105	HOMO→LUMO +1 (97.5%)
M6	1015.46	1.2210	1.5757	HOMO→LUMO +1 (99.1%)

Discussion

Geometrical optimization

Techniques for determining the three dimensional atomic configuration of a molecule by lowering model energy is known as geometry optimization. In order to optimize geometry aimed at M1, M2, M3, M4, M5 and M6, the B3LYP/6-311G basis set was utilized. Selected geometrical parameters such as dihedral angles were taken into consideration in order to assess the conformation of the dye molecules under study. Figure 2, displays the optimum structure for each dye molecule that was investigated in solvent phases and the trends are similar even in gas phase. Additionally, Table 1 shows the selected dihedral angles that were obtained from the optimum geometries. According to their optimum structures, which are displayed in Figure 2, it was discovered that each dye molecule under study had an identical planar conformation in its optimal geometries. This assessed by dihedral angle values of all studied dye molecules that were ranging from nearly 180° and indicates planar conformation. Thus by altering internal acceptors, the molecules were twisted owing towards steric connections between the inserted acceptor and π-spacer hence become more effective at absorbing (Liang and Chen, 2013).

Frontier molecular orbitals

Key information about the optoelectronic properties of dyes is provided by quantum mechanical descriptors called frontier molecular orbitals (FMOs) which is comprising of HOMO and LUMO (Adnan *et al.,* 2017). These orbitals facilitate the study of distribution and stabilization of the charge density across the molecules. However, FMOs are essential for figuring out the dye molecules' ICT as well as charge separated-states (Khalid *et al.,* 2021). The contour plots of the HOMO and LUMO orbitals of the dye molecules under examination are displayed in Figure 3 as computed in solvent phase and the trends are similar even in gas phase following geometries optimization. According to the FMOs study, the HOMO electrons for all considered dyes M1-M6 were widely distributed on electron rich side, with maximal densities on the donor and minimal densities on the internal acceptor. On the other hand, the LUMO electrons were more extensively dispersed on electron deficient side with maximal densities on the external acceptor and π-spacer and minimal densities on the internal acceptor. The FMOs result typically displays that the HOMO is placed at the donor group and LUMO is mostly placed at the external acceptor group as well as π-spacer. From this, it can be inferred that the designed D-A'-π-A system is successful as the electron can spontaneously move from the donor group to the acceptor group. Furthermore, the scenario indicates that the oxygen and nitrogen atoms of the external acceptors serve as the anchoring groups to semiconductor for all designed dye molecules, despite the possibility that the same atoms from the π-spacer may also strengthening the performance by participating in anchoring.

The HOMO and LUMO energies determine the effective transferring of charge concerning the donor and acceptor. The proper energy level of photosensitizer material is necessary aimed at electron injection as well as material regeneration, as per the operating principle of DSSCs. In order to encourage dye regeneration and prevent charge recombination between the photoinjected electron and the oxidized organic dye, the HOMO energy levels must be below the -4.8 eV electrolyte redox potential, while the LUMO energy levels must be above the -4.0 eV of TiO_2 conduction band (CB) edge. This indicates a strong thermodynamic driving force for efficient electron injection from the excited state of dye to the semiconductor's conduction band (Azaid *et al.,* 2022). The information shown in Table 2 clearly shows that, in both the gas and solvent phases, the dye sensitizers' HOMO energy levels are in the following order: M2 (-5.1111 eV) > M4 (-5.1557 eV) > M1 (-5.1843 eV) > M3 (-5.2725 eV) > M6 (-5.3536 eV) > M5 (-5.4548 eV) and M2 (-4.9669 eV) > M1 (-5.0281 eV) > M4 (-5.0316 eV) > M3 (-5.0983 eV) > M6 (-5.2151 eV) > M5 (-5.2877 eV), respectively. The data indicated a high level of performance and regeneration potential. Consequently, M2 is more capable of regeneration than other dye molecules. However, the LUMO energy levels for gas and solvent phases, respectively, are arranged in the order of M5 (-3.9307 eV) > M6 (-3.8893 eV) > M3 (-3.8463 eV) > M4 (-3.7726 eV) > M1 (-3.7239 eV) > M2 (-3.6997 eV) and M5 (-3.9143 eV) > M6 (-3.8678 eV)

> M3 (-3.8656 eV) > M4 (-3.8100 eV) > M1 (-3.7784 eV) > M2 (-3.7484 eV). These values suggest an injection capability. Thus, M5 can easily inject electrons to conduction band than other dye molecules. Due to its small difference in regeneration value of 0.1659 eV rather than the large difference in injection value of 0.3437 eV, M2 is expected to perform better than M5 in ICT.

Narrow bandgap energy sensitizers are better suitable for electron excitation and have superior absorption properties. Thus, molecule activity is greatly impacted by the energy gap. Because of this, sensitizers may absorb more visible light, raising the J_{SC} and PCE (Muñoz-García *et al.*, 2021). Table 2, showed the energy bandgap of dye molecules for gas and solvent phases, respectively, in the following order: M4 (-1.3831 eV) < M2 (-1.4114 eV) < M3 (-1.4262 eV) < M1 (-1.4604 eV) < M6 (-1.4643 eV) < M5 (-1.5241 eV) and M2 (-1.2185 eV) < M4 (-1.2216 eV) < M3 (-1.2327 eV) < M1 (-1.2542 eV) < M6 (-1.3473 eV) < M5 (-1.3734 eV). The results revealed in Table 2 indicate that M2 and M4 exhibited smaller energy bandgaps than other dye molecules in both the gas and solvent phases, indicating that they would perform better in terms of reactivity and J_{SC} than other dye molecules.

The electronic charge distribution of the dye molecule is symmetry as seen by the dipole moment presented in Table 2. It is crucial to keep in mind that an increased dipole moment is associated with asymmetric behavior in the electronic charge distribution, which makes molecules more sensitive and vulnerable toward external electric field (El Assyry *et al.*, 2015). Based on the Table 2, the dipole moment order in the gas and solvent phases is as follows: M1 (15.6729) < M4 (16.3504) < M3 (16.5103) < M5 (17.8410) < M2 (18.1707) < M6 (18.2094) and M1 (21.6061) < M4 (23.4206) < M2 (23.9170) < M3 (24.8342) < M6 (25.9480) < M5 (27.4097), respectively. In the gas phase, M2 and M6 generally had greater dipole moments than other dye molecules, while in the solvent phase M5 and M6 had larger dipole moments than the other dyes. As a result, dye molecule M6 is more sensitive toward the external electric field.

Photovoltaic properties

The considerations presented in Table 3 shows the photovoltaic characteristics of the calculated dye molecules. The electronic injection-free energy (ΔG^{inject}), dye's ground state oxidation potential energy (E^{dye}), excited state oxidation potential energy (E^{dye^+}), open-circuit voltage (V_{OC}) and light-harvesting efficiency (LHE) are all included in the previously mentioned metrics. The dye's ability to absorb solar photons as well as introduce photoexcited electrons from the LUMO into the CB is explained by these crucial variables. With the exception of M5, all dye molecules have negative values of ΔG^{inject}, signifying that the process of electron injection is spontaneous. Furthermore, all dye molecules (except from M5) have an excited state that is located above the CB of the semiconductor, indicating high electron injection efficiency from the excited to the TiO_2 CB. The M2 (-0.1807 eV) > M1 (-0.1581 eV) > M4 (-0.1225 eV) > M3 (-0.0720 eV) > M6 (-0.0201 eV) > M5 (0.0012 eV) is the order in which the electron injection efficiency values are organized in gas phase, and M2 (-0.1125 eV) > M1 (-0.0858 eV) > M4 (-0.0685 eV) > M3 (-0.0269 eV) > M6 (-0.0059 eV) > M5 (0.0248 eV) in the solvent phase. The findings indicate that M2 exhibits a greater value of ΔG^{inject} for both gas and solvent phases. This suggests that there is a high electron injection efficiency due to thermodynamically favorable electron injection from dyes into the TiO_2 semiconductor. However, dye molecule M5 with non-spontaneous injection power confirmed to be not applicable in DSSCs technology despite of having extraordinary performance in other properties like ICT.

Table 3, displays the LHE values of all dye molecules in the following order: M5 (0.9748) > M3 (0.9581) > M6 (0.9554) > M4 (0.9355) > M1 (0.9193) > M2 (0.9153) and M5 (0.9845) > M3 (0.9766) > M6 (0.9734) > M4 (0.9677) > M1 (0.9430) > M2 (0.9319) in the gas phase and solvent phase, respectively. The variations in LHE values are due to the attachment of various internal acceptors to the donor group. Consequently, M3 dye molecule has higher LHE value than other dye molecules, and it shows promise as a dye molecule for use in DSSCs. However, in results show that M5 dye molecule has greater value of LHE of 0.9748 in gas phase and 0.9845 in solvent phase but was not considered to be favorable candidate in DSSCs application because of its

inability to inject electron to the semiconductor and become non-spontaneous molecule that's why M3 dye molecule take advantage to be recommended as a favorable candidate for use in the application of DSSCs. With an increase in oscillator strength, light harvesting, electron injection and J_{SC} become more efficient. To accomplish quick electron transport, electronic regeneration-free energy (ΔG_{reg}) must be as low as practical. Table 3 demonstrates the trend of ΔG_{reg} in the order of M2 (0.3111 eV) < M4 (0.3557 eV) < M1 (0.3843 eV) < M3 (0.4725 eV) < M6 (0.5536 eV) < M5 (0.6548 eV) and M2 (0.1689 eV) < M1 (0.2281 eV) < M4 (0.2316 eV) < M3 (0.2983 eV) < M6 (0.4151 eV) < M5 (0.4877 eV) in the both gas phase and solvent phase, respectively. According to the findings, the M2 dye molecule had lower ΔG_{reg} value than other dye molecules which implies greater power conversion efficiency (η).

The open-circuit voltage (V_{OC}) parameter is also measure to ascertain the DSSC power conversion efficiency and a greater value of V_{OC} in molecular dye indicates a higher electron injection power. Table 3, provides more information about the declining trends in V_{OC} in the gas phase M2 (0.3003 eV) < M1 (0.2761 eV) < M4 (0.2274 eV) < M3 (0.1573 eV) < M6 (0.1107 eV) < M5 (0.0693 eV) and in solvent phase M2 (0.2516 eV) < M1 (0.2216 eV) < M4 (0.1900 eV) < M3 (0.1344 eV) < M6 (0.1322 eV) < M5 (0.0857 eV). The results showed that, for both gas phase and solvent phase, respectively, the M2 dye molecule had a higher V_{OC} value than the other dye molecules. In light of the fact that V_{OC} and η are strongly correlated, M2 dye recommended to be used more often in DSSCs application due to its higher power conversion efficiency in practical use.

Absorption properties

In order to analyze the dyes' absorption behavior, the transition energy, oscillator strength (f) and vertical excited singlet state of each dye molecule in the gas and solvent phases was investigated. Normally, dyes with larger absorption bands and higher absorption strengths are more effective. Table 4 lists all dye molecules along with their calculated maximum wavelength (λ_{max}), transition energy (HOMO to LUMO), transition character (TC %) and computed vertical excitation (E_{ex}). The sequence of the first vertical excited state increases as follows: M4 < M2 < M1 < M3 < M6 < M5 in gas phase while in solvent phase it is M2 < M4 < M1 < M3 < M6 < M5. The results show that in gas and solvent phase, M5 and M6 perform better in vertical excitation energy than other dye molecules.

There exists a strong correlation between the oscillator strength (f) and light-harvesting efficiency. In both the gas and solvent phases, the oscillator strengths of all dye molecules are organized as follows: M5 > M3 > M6 > M4 > M1 > M2. As a result, compared to other dye molecules, M5 and M3 dye molecules showed greater strengths in the gas as well as solvent phases, and this suggests that it will function better and boost DSSC application efficiency. From Table 4 and Figure 4, the values of maximum absorption wavelength are shown. In gas and solvent phases, respectively, the maximum absorption wavelength of all dye molecules under investigation decrease in the following order: M4 (969.96 nm) > M2 (959.76 nm) > M3 (922.17 nm) > M1 (923.58 nm) > M6 (900.00 nm) > M5 (852.96 nm) and M2 (1148.59 nm) > M4 (1127.04 nm) > M1 (1113.04 nm) > M3 (1101.85 nm) > M6 (1015.46 nm) > M5 (981.76 nm). The results show that compared to other dye molecules, M2 and M4 have greater maximum absorption wavelengths in both the gas and solvent phases. Due to their longer wavelengths and red shift, M2 and M4 dye molecules are the most recommended choice for DSSC applications.

Overall, M2 outperformed other dye molecules because of the little differences in their properties, such as the 0.5259 oscillator strength difference and the 0.1618 eV vertical excitation energy difference between M5 and M2 and in comparison of worse performance of M5 in other parameters like injection power. However, the significant difference between M5 and M2 in maximum absorption wavelength of 107.80 nm makes M2 a more effective dye molecule than others, and it may even prove to be a good choice for DSSC application.

Conclusion

In this study, Using DFT and TD-DFT techniques six series of novel organic dye with D-A'-π-A

framework and six various internal acceptors were successful designed and examined. Findings show that it is possible to adjust the molecular dyes to the desired photovoltaic characteristics by varying internal acceptor. The analysis of optimal geometries, photovoltaic properties, absorption properties and charge transfer capacity were investigated to find possible sensitizers that can be used in solar cells. In general, M2 dye molecule was performed better than other dye molecules due to its higher value of V_{OC} of 0.3003 eV and 0.2516 eV for gas and solvent, respectively, large value of ΔG^{inject} of -0.1807 eV and -0.1125 eV for gas and solvent phase and maximum absorption wavelength of 959.76 nm and 1148.69 nm for gas and solvent phase, respectively. Therefore, M2 dye molecule becomes more favorable candidate for the application of DSSCs. Also, this contribution can offer effective direction for developing D-A′-π-A organic dye for DSSCs.

Recommendation

Computational studies were primarily concerned with the theoretical approximation of electronic, optical, and molecular systems. Out of all the designed molecules, the M2 dye molecule showed the most promise for application in DSSCs based on theoretical calculations. To ensure that the M2 dye molecule is effective in real-world applications, more synthesis research is necessary. Computational and experimental approaches are also needed to confirm the dye molecule's applicability and efficacy. Confessing computational chemistry as a valuable subject for molecular modeling is crucial. It is preferable to employ computational approaches prior to conducting tests since they offer knowledge that supplements experimental data.

Acknowledgement

We would like to thank the crews in the department of chemistry and computational laboratory at the University of Dodoma for support to accomplish this work.

References

Abusaif, M. S., Fathy, M., Abu-Saied, M. A., Elhenawy, A. A., Kashyout, A. B., Selim, M. R., & Ammar, Y. A. (2021). New carbazole-based organic dyes with different acceptors for dye-sensitized solar cells: Synthesis, characterization, dssc fabrications and density functional theory studies. *Journal of Molecular Structure*, *1225*, 129297.

Adnan, M., Iqbal, J., Bibi, S., Hussain, R., Akhtar, M. N., Rashid, M. A., Eliasson, B., & Ayub, K. (2017). Fine Tuning the Optoelectronic Properties of Triphenylamine Based Donor Molecules for Organic Solar Cells. *Zeitschrift Fur Physikalische Chemie*, *231*(6), 1127–1139.

Al-Masoodi1, K. O. K., Rafiq, I., Assyry, A. El, & Derouiche, A. (2021). DFT / TD-DFT Study of Donorπ-Acceptor Organic Dye models contained Triarylamine for an Efficient Dye-Sensitized Solar Cell DFT / TD-DFT Study of Donor - π - Acceptor Organic Dye models contained Triarylamine for an Efficient Dye-Sensitized Solar Cell. *Journal of Physics: Conference Series*.

Arslan, B. S., Arkan, B., Gezgin, M., Derin, Y., Avcı, D., Tutar, A., Nebioğlu, M., & Şişman, İ. (2021). The improvement of photovoltaic performance of quinoline-based dye-sensitized solar cells by modification of the auxiliary acceptors. *Journal of Photochemistry and Photobiology A: Chemistry*, *404*(September 2020), 1–10.

Azaid, A., Raftani, M., Alaqarbeh, M., & Kacimi, R. (2022). *New organic dye-sensitized solar cells based on the D – A – p – A structure for e ffi cient DSSCs : DFT / TD- DFT investigations*. *c*, 30626–30638.

Bouzzine, S. M., Abdelaaziz, A., Hamidi, M., Al-Zahrani, F. A. M., Zayed, M. E. M., & El-Shishtawy, R. M. (2023). The Impact of TPA Auxiliary Donor and the π-Linkers on the Performance of Newly Designed Dye-Sensitized Solar Cells: Computational Investigation. *Materials*, *16*(4).

Chaitanya, K., Heron, B. M., & Ju, X. H. (2017). Influence of a local electric field on the light harvesting efficiency of a cyclopentadithiophene-bridged D-A-π-A indoline dye on pure and N-doped TiO2 surfaces. In *Dyes and Pigments* (Vol. 141). Elsevier Ltd.

Chen, C. Y., Wang, M., Li, J. Y., Pootrakulchote, N., Alibabaei, L., Ngoc-Le, C. H., Decoppet,

J. D., Tsai, J. H., Grätzel, C., Wu, C. G., Zakeeruddin, S. M., & Grätzel, M. (2009). Highly efficient light-harvesting ruthenium sensitizer for thin-film dye-sensitized solar cells. *ACS Nano*, *3*(10), 3103–3109.

Chenab, K. K., & Zamani-Meymian, M. R. (2022). Developing efficient dye-sensitized solar cells by inclusion of ferrocene and benzene π-bridges into molecular structures of triphenylamine dyes. *Materials Science in Semiconductor Processing*, *151*(August), 107018.

Cossi, M., & Barone, V. (2001). Time-dependent density functional theory for molecules in liquid solutions. *Journal of Chemical Physics*, *115*(10), 4708–4717.

Cui, L., Zhou, J., Zhang, Y., Meng, X., Wang, H., & Liu, B. (2023). Dyes and Pigments Molecular engineering of auxiliary acceptor for the development of efficient organic D-A- π -A sensitizers. *Dyes and Pigments*, *216*(January), 111322.

Dindorkar, S. S., & Yadav, A. (2022). Insights from Density Functional Theory on the Feasibility of Modified Reactive Dyes as Dye Sensitizers in Dye-Sensitized Solar Cell Applications. *Solar*, *2*(1), 12–31.

dos Santos, G. C., Oliveira, E. F., Lavarda, F. C., & da Silva-Filho, L. C. (2019). Designing new quinoline-based organic photosensitizers for dye-sensitized solar cells (DSSC): a theoretical investigation. *Journal of Molecular Modeling*, *25*(3).

El Assyry, A., Jdaa, R., Benali, B., Addou, M., & Zarrouk, A. (2015). Optical and photovoltaic properties of new quinoxalin-2(1H)-one-based D-A organic dyes for efficient dye-sensitized solar cell using DFT. *Journal of Materials and Environmental Science*, *6*(9), 2612–2623.

Fernandes, S. S. M., Castro, M. C. R., Ivanou, D., Mendes, A., & Raposo, M. M. M. (2022). Push-Pull Heterocyclic Dyes Based on Pyrrole and Thiophene: Synthesis and Evaluation of Their Optical, Redox and Photovoltaic Properties. *Coatings*, *12*(1).

Frisch, M. J., Trucks, G. W., Schlegel, H. B., Scuseria, G. E., Robb, A., Cheeseman, J. R., Scalmani, G., Barone, V., Mennucci, B., Petersson, G. A., Caricato, M., Li, X., Hratchian, H. P., Izmaylov, A. F., Bloino, J., Zheng, G., Hada, M., Ehara, M., Toyota, K., … Ct, W. (2015). *Gaussian 09, Revision*. 1–20.

Hachi, M., Slimi, A., Benjelloun, A. T., Fitri, A., Elkhattabi, S., & Benzakour, M. (2020). The influence of the structural variations in the π-bridge of D-π-A organic dyes on the efficiency of dye-sensitized solar cells (DSSCs): A DFT computational study. *2020 5th International Conference on Renewable Energies for Developing Countries, REDEC 2020*, *5*.

Hosseinnezhad, M., Gharanjig, K., Yazdi, M. K., Zarrintaj, P., Moradian, S., Saeb, M. R., & Stadler, F. J. (2020). Dye-sensitized solar cells based on natural photosensitizers: A green view from Iran. *Journal of Alloys and Compounds*, *828*, 154329.

Huang, H., Chen, H., Long, J., Wang, G., & Tan, S. (2016). Novel D e A e p e A organic dyes based on 3-dimensional triarylamine and benzothiadiazole derivatives for high-performance dye-sensitized solar cells. *Journal of Power Sources*, *326*, 438–446.

Janjua, M. R. S. A., Khan, M. U., Khalid, M., Ullah, N., Kalgaonkar, R., Alnoaimi, K., Baqader, N., & Jamil, S. (2021). Theoretical and Conceptual Framework to Design Efficient Dye-Sensitized Solar Cells (DSSCs): Molecular Engineering by DFT Method. *Journal of Cluster Science*, *32*(2), 243–253.

Jungsuttiwong, S., Tarsang, R., Sudyoadsuk, T., Promarak, V., Khongpracha, P., & Namuangruk, S. (2013). Theoretical study on novel double donor-based dyes used in high efficient dye-sensitized solar cells: The application of TDDFT study to the electron injection process. *Organic Electronics*, *14*(3), 711–722.

Kacimi, R., Bourass, M., Toupance, T., Wazzan, N., Chemek, M., El, A., Lahcen, A., & Kamel, B. (2020). Computational design of new organic (D – π – A) dyes based on benzothiadiazole for photovoltaic applications , especially dye - sensitized solar cells. *Research on Chemical Intermediates*, *0123456789*.

Katoh, R., Furube, A., Yoshihara, T., Hara, K., Fujihashi, G., Takano, S., Murata, S., Arakawa, H., & Tachiya, M. (2004). *Efficiencies of Electron Injection from Excited N3 Dye into Nanocrystalline Semiconductor*. 4818–4822.

Khalid, M., Khan, M. U., Shafiq, I., Hussain, R.,

Ali, A., Imran, M., Braga, A. A. C., Fayyaz Ur Rehman, M., & Akram, M. S. (2021). Structural modulation of π-conjugated linkers in D-π-A dyes based on triphenylamine dicyanovinylene framework to explore the NLO properties. *Royal Society Open Science*, *8*(8).

Kim, B. G., Chung, K., & Kim, J. (2013). Molecular design principle of all-organic dyes for dye-sensitized solar cells. *Chemistry - A European Journal*, *19*(17), 5220–5230.

Li, Y., Liu, J., Liu, D., Li, X., & Xu, Y. (2019). D-A-π-A based organic dyes for efficient DSSCs : A theoretical study on the role of π-spacer. *Computational Materials Science*, *161*(January), 163–176.

Liang, M., & Chen, J. (2013). Arylamine organic dyes for dye-sensitized solar cells. In *Chemical Society Reviews* (Vol. 42, Issue 8).

Liu, P., Sharmoukh, W., Xu, B., Li, Y. Y., Boschloo, G., Sun, L., & Kloo, L. (2017). *Novel and Stable D − A − π − A Dyes for E ffi cient Solid-State Dye- Sensitized Solar Cells*.

Mathew, S., Yella, A., Gao, P., Humphry-Baker, R., Curchod, B. F. E., Ashari-Astani, N., Tavernelli, I., Rothlisberger, U., Nazeeruddin, M. K., & Grätzel, M. (2014). Dye-sensitized solar cells with 13% efficiency achieved through the molecular engineering of porphyrin sensitizers. *Nature Chemistry*, *6*(3), 242–247.

Muñoz-García, A. B., Benesperi, I., Boschloo, G., Concepcion, J. J., Delcamp, J. H., Gibson, E. A., Meyer, G. J., Pavone, M., Pettersson, H., Hagfeldt, A., & Freitag, M. (2021). Dye-sensitized solar cells strike back. *Chemical Society Reviews*, *50*(22), 12450–12550.

Ndiaye, A., Dioum, A., Oprea, C. I., Dumbrava, A., Lungu, J., Georgescu, A., Moscalu, F., Gîrțu, M. A., Beye, A. C., & Youm, I. (2021). A Combined Experimental and Computational Study of Chrysanthemin as a Pigment for Dye-Sensitized Solar Cells. *Molecules*, *26*(1), 1–15.

Pizzicato, B., Pacifico, S., Cayuela, D., Mijas, G., & Riba-Moliner, M. (2023). Advancements in Sustainable Natural Dyes for Textile Applications: A Review. *Molecules*, *28*(16), 1–22.

Pounraj, P. (2018). *Donor functionalized quinoline based organic sensitizers for dye sensitized solar cell (DSSC) applications : DFT and TD-DFT investigations*.

Prajapat, K., Dhonde, M., Sahu, K., Bhojane, P., Murty, V. V. S., & Shirage, P. M. (2023). The evolution of organic materials for efficient dye-sensitized solar cells. *Journal of Photochemistry and Photobiology C: Photochemistry Reviews*, *55*(April), 100586.

Saad Ebied, M., Dongol, M., Ibrahim, M., Nassary, M., Elnobi, S., & Abuelwafa, A. A. (2022). Effect of carboxylic acid and cyanoacrylic acid as anchoring groups on Coumarin 6 dye for dye-sensitized solar cells: DFT and TD-DFT study. *Structural Chemistry*, *33*(6), 1921–1933.

Sharmoukh, W., Cong, J., Ali, B. A., Allam, N. K., & Kloo, L. (2020). Comparison between Benzothiadizole-Thiophene-and Benzothiadizole-Furan-Based D-A-Ï€-A Dyes Applied in Dye-Sensitized Solar Cells: Experimental and Theoretical Insights. *ACS Omega*, *5*(27), 16856–16864.

Sharmoukh, W., Hassan, Z. M., Ali, B. A., & Elnagar, M. M. (2018). Journal of Photochemistry & Photobiology A : Chemistry Position of the anchoring group determined the sensitization e ffi ciency of metal-free D- π -A dyes : Combined experimental and TD – DFT insights. *Journal of Photochemistry & Photobiology, A: Chemistry*, *367*(June), 128–136.

Singh, P., & Ravindra, N. M. (2012). Solar Energy Materials & Solar Cells Temperature dependence of solar cell performance — an analysis. *Solar Energy Materials and Solar Cells*, *101*, 36–45.

Slimi, A., Fitri, A., Benjelloun, A. T., Elkhattabi, S., Benzakour, M., Mcharfi, M., & Bouachrine, M. (2019). *Molecular Design of D- p -A-A Organic Dyes Based on Triphenylamine Derivatives with Various Auxiliary Acceptors for High Performance DSSCs*.

Tingare, Y. S., Su, C., Shen, M. T., Tsai, S. H., Ho, S. Y., & Li, W. R. (2020). New oxindole-bridged acceptors for organic sensitizers: Substitution and performance studies in dye-sensitized solar cells. *Molecules*, *25*(9), 40–42.

Tripathi, A., Ganjoo, A., & Chetti, P. (2020). *Influence of internal acceptor and thiophene based π -spacer in D-A- π -A system on photophysical and charge transport properties*

for efficient DSSCs : A DFT insight. *209*(September), 194–205.

Vuai, S. A. H., Khalfan, M. S., & Babu, N. S. (2021). DFT and TD-DFT studies for optoelectronic properties of coumarin based donor-π-acceptor (D-π-A) dyes: applications in dye-sensitized solar cells (DSSCS). *Heliyon*, *7*(11), e08339.

Wang, X., Xu, J., Li, M., Fang, D., Chen, B., Wang, L., & Xu, W. (2013). Highly efficient unsymmetrical squaraines for panchromatic dye-sensitized solar cells: A computational study. *RSC Advances*, *3*(15), 5227–5237.

Wu, H., Huang, Z., Hua, T., Liao, C., Meier, H., Tang, H., Wang, L., & Cao, D. (2019). Metal-free organic dyes with di(1-benzothieno)[3,2-b:2′,3′-d]pyrrole as a donor for efficient dye-sensitized solar cells: Effect of mono- and bi-anchors on photovoltaic performance. *Dyes and Pigments*, *165*(February), 103–111.

Zhang, T., Guan, W., Wen, S., Yan, L., & Su, Z. (2014). *Theoretical Studies on Metalloporphyrin − Polyoxometalates Hybrid Complexes for Dye-Sensitized Solar Cells*. 2–7.

Zhang, X., Gou, F., Zhao, D., Shi, J., Gao, H., Zhu, Z., & Jing, H. (2016). π-Spacer effect in dithiafulvenyl-π-phenothiazine dyes for dye-sensitized solar cells. *Journal of Power Sources*, *324*, 484–491.

Zuo, X., Chang, K., Zhao, J., Xie, Z., Tang, H., Li, B., & Chang, Z. (2015). Bubble-Template-Assisted Synthesis of Hollow Fullerene-Like MoS2 Nanocages as a Lithium Ion Battery Anode Material Xiaoxia. *Journal of Materials Chemistry A*.